Recent progress in upgrading metallurgical-grade silicon to solar-grade silicon via pyrometallurgical routes

Reference:

Y. Lei; X. Ma; Y. Wang, et al., Recent progress in upgrading metallurgical-grade silicon to solar-grade silicon via pyrometallurgical routes. International Journal of Minerals, Metallurgy and Materials 2022, 29 (4), 767-782.

ISSN 1869-103X (2022), Copyright © 2022 University of Science and Technology Beijing. All rights reserved
Full text (Publisher's DOI): https://doi.org/10.1007/s12613-022-2418-3
Received 07 October 2021; Received in revised form 17 December 2021; Accepted 17 January 2022

Recent progress in upgrading metallurgical-grade silicon to solar-grade silicon via pyrometallurgical routes

Yun Lei[1)], Xiaodong Ma[2)], Ye Wang[3)], Zhiyuan Chen[4)], Yongsheng Ren[1)], Wenhui Ma[1)], Kazuki Morita[5)*]

1) Faculty of Metallurgical and Energy Engineering/State Key Laboratory of Complex Non-Ferrous Metal Resources Clean Utilization, Kunming University of Science and

Technology, Kunming 650093, China

2) Sustainable Minerals Institute, The University of Queensland, St Lucia, 4072, QLD, Australia.

3) School of Chemical Engineering, Sichuan University, Chengdu, 610065, Sichuan, China

4) Separation and Conversion Technology, Flemish Institute for Technological Research, 2400, Mol, Belgium.

5) Department of Materials Engineering, Graduate School of Engineering, The University of Tokyo, 7-3-1 Hongo, Bunkyo-ku, Tokyo 113-8656, Japan

[*] Corresponding authors: Kazuki Morita, E-mail: kzmorita@material.t.u-kyo.ac.jp

Abstract

The Si-based photovoltaic industry is developing rapidly as a renewable and green energy source. The widespread use of Si-based solar cells requires large amounts of solar-grade Si (SoG-Si) to manufacture Si wafers. Chemical routes, mainly the modified Siemens process, have dominated the market ; however, as a series of complex chemical reactions and various corrosive and hazardous reagents are involved in traditional chemical techniques, large amounts of complex waste solar cells and Si kerf slurry waste are gradually accumulating and are difficult to recycle using traditional chemical techniques, and new techniques are required to meet the SoG-Si preparation and Si waste recycling demands. The metallurgical route is a promising route; however, eliminating B and P from metallurgical-grade Si (MG-Si) is a bottleneck problem. Various pyrometallurgical treatments have been proposed to enhance the removal of B and P from MG-Si. This article reviews Si refining with slag treatment, chlorination, vacuum evaporation, and solvent refining, and summarizes and discusses the basic principles and recent representative studies of the four methods. Solvent refining is the most promising and environmentally friendly approach for obtaining low-cost SoG-Si and is a popular research topic. Finally, a pure physical, simple, and green approach, that is, a combination of solvent refining, slag treatment, or vacuum directional solidification, is proposed to prepare low-cost SoG-Si using MG-Si or Si wastes as raw materials.

Keywords: please insert keywords

1. Introduction

With the ever reducing availability of fossil fuels and the increasing attention on global environmental problems, renewable and clean energies have rapidly developed in recent years. Solar energy is a typical example. Although many new non-Si-based solar cells have been proposed, Si-wafer-based solar cells accounted for 95% of the total global solar cell production in 2020 **[1]**. As even a small quantity of impurities in the Si wafer can significantly decrease the photoelectric conversion efficiency of solar cells, the total concentration of impurities in Si must be controlled to an extremely low level. The purity of the Si employed for preparing Si wafers must be 99.9999% (with a total of 1 ppmw of impurities) and is referred to as solar-grade Si (SoG-Si). **Table 1** lists the acceptable contamination levels of impurities in SoG-Si, as reported in the literature **[2,3]**, and the effects of the said impurities on the photoelectric conversion efficiency **[4]**. Two types of SoG-Si, namely, multi-Si and mono-Si, are used as raw materials for preparing Si wafers. Multi-Si was the dominant raw material for preparing Si wafers from 2000 to 2018, while mono-Si has been the dominant raw material since 2019 because of its sharp decrease in cost **[1]**. However, regardless of whether multi-Si or mono-Si is used, metallurgical-grade Si (MG-Si; purity is normally below 99.5%) is the raw material used for the preparation of SoG-Si. **Table 1** lists the main impurities in MG-Si as reported in the MG-Si compositions presented in references **[5-9]**.

Table 1. The main impurities in MG-Si and SoG-Si **[2-9]**.

Element	MG-Si, ppmw	SoG-Si, ppmw
Si	98–99.5%	>99.9999%
Fe	200–4000	<0.0097
Ca	30–500	<1

Al	200–1800	<0.1
Ti	100–300	<0.00027
C	<1700	<5
Cu	30–60	<0.0059
Mn	30–300	<0.01
Cr	4–60	<0.00047
V	10–300	<0.005
B	8–70	<1.5
Zr	<20	<0.0001
Ni	20–220	<0.1
P	20–250	<1

The modified Siemens process is currently the dominant method for preparing SoG-Si. However, as a chemical route, the modified Siemens process involves a series of complex chemical reaction steps and various corrosive and hazardous chloride reagents making this process less environmentally friendly and economical. Additionally, with the fast-growing global photovoltaic industry (the compound annual growth rate of cumulative PV installations was 34% between 2010 and 2020 **[1]**), large amounts of complex Si waste, such as spent Si-based solar cells and Si kerf slurry waste, is inevitably accumulating. These complex Si wastes are not easily recycled by conventional chemical routes because they normally contain high levels of O (Si kerf slurry waste), adhesives, and glasses (spent solar cells). Therefore, new alternative approaches are necessary, not only for upgrading MG-Si to SoG-Si but also for recycling Si waste generated by the photovoltaic industry. Metallurgical routes have been proposed and have developed quickly because of their cost and environmental advantages and are becoming the most promising routes because they can prepare SoG-Si and recycle Si wastes.

The metallurgical route includes hydrometallurgical and pyrometallurgical treatments, such as slag treatment, vacuum evaporation, plasma treatment, electron beam melting, chlorination, directional solidification, and solvent refining. Hydrometallurgical treatment can eliminate impurities agglomerated at the grain boundary of MG-Si crystals, but can scarcely eliminate impurities dissolved in the MG-Si crystals, particularly those impurities with a large solubility in solid Si, such as Al, B, Sn, and P. Xi *et al.* **[10]** reviewed hydrometallurgical techniques for the removal of impurities from MG-Si. Similar to hydrometallurgical treatments, impurities which have a low solubility in solid Si (or small segregation coefficients in Si) can be easily eliminated by directional solidification. However, directional solidification can hardly eliminate impurities with large segregation coefficients in Si, especially B and P impurities. Therefore, eliminating impurities, especially B and P, is a bottleneck problem that requires resolution by the metallurgical route. Slag treatment, vacuum evaporation, plasma treatment, electron beam melting, chlorination, and solvent refining have been proposed to eliminate B and P from MG-Si. The application of plasma treatment and electron beam melting is limited because of their high cost and energy consumption. This article reviews the research progress of Si refining at high temperatures using slag treatment, chlorination, vacuum evaporation, and solvent refining. Finally, a pure physical process for Si refining and Si waste recycling is proposed, which may guide the development of a new metallurgical route.

2. Slag treatment

Slag treatment is mainly used to eliminate B from Si because B cannot be effectively eliminated by conventional approaches, such as directional crystallization, vacuum evaporation, and hydrometallurgy.

Figure 1 presents a schematic diagram of B removal by the slag treatment process **[11]**, in which the basic principle is that the affinity of B for O is stronger than that of Si for O, as expressed in **Eq. (1)**.

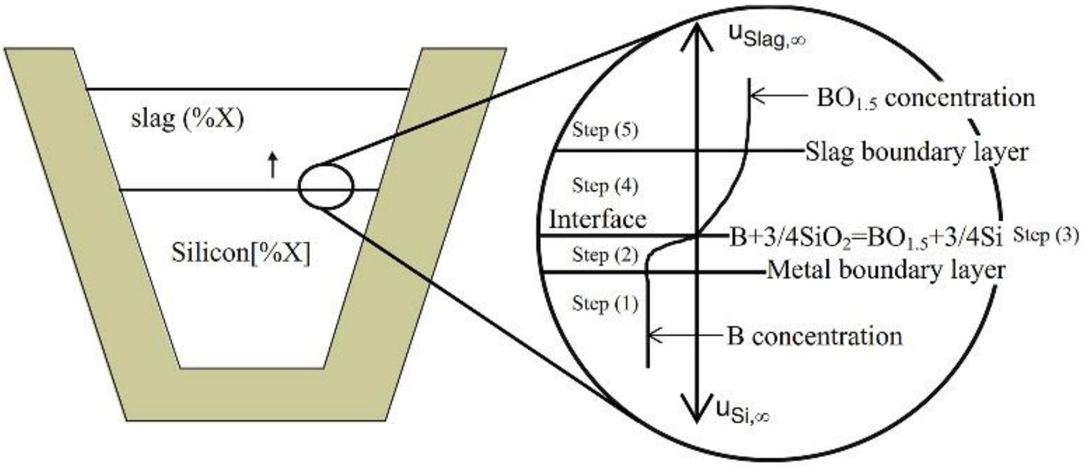

Fig. 1. Reaction mechanism of the removal of B using CaO-SiO_2 slag **[11].**

$$\mathrm{B(l)} + \frac{3}{4}\mathrm{SiO_2(l)} = \mathrm{BO_{1.5}(l)} + \frac{3}{4}\mathrm{Si(l)} \tag{1}$$

The B distribution ratio (L_B, that is, the concentration ratio of B in molten slag to that in Si) is often used to characterize the removal effect of B. A larger L_B value indicates a larger B removal ratio. L_B is expressed as:

$$L_\mathrm{B} = \frac{x_{\mathrm{BO_{1.5}\ in\ slag}}}{x_{\mathrm{B\ in\ Si\ melt}}} = K \cdot \frac{\gamma_\mathrm{B} \cdot a_{\mathrm{SiO_2}}^{3/4}}{\gamma_{\mathrm{BO_{1.5}}} \cdot a_{\mathrm{Si}}^{3/4}} \tag{2}$$

According to **Eq. (2)**, to enhance the removal of B, that is, increase the value of L_B, the value of γ_B or $a_{\mathrm{SiO_2}}$ should be increased or the value of $\gamma_{\mathrm{BO_{1.5}}}$ or a_{Si} should be decreased. The oxidation of B by the oxide slag can be expressed by **Eq. (3)**:

$$B + \frac{3}{4}O_2 + \frac{3}{2}O^{2-} = BO_3^{3-} \qquad (3)$$

A good separation between the molten slag and the Si melt can yield bulk Si. The Si-slag separation is affected by the viscosity **[12]** and density **[13]** of the slag, and the Si-slag interfacial tension **[14]**. Slags with a low melting point, low viscosity, large Si-slag density difference, and sufficient free O are also important for obtaining a large L_B.

Table 2 summarizes the relevant research results for refining MG-Si by slag treatment. CaO-SiO_2 is the most basic and widely used binary slag system for the research and application of MG-Si slag treatment processes **[15–18]**. To improve L_B and obtain bulk Si, ternary and multicomponent slag systems, or other binary slag systems that can reduce the viscosity and melting point, have gradually become popular research topics. Cai *et al.* **[48]** found that adding CaF_2 introduced F^-, which reduces the viscosity of the slag, improving the slag melt fluidity. Introducing Na_2O/K_2O or Na_2CO_3/K_2CO_3, oxides with higher oxidization abilities than CaO, can increase the L_B value. The dissolved B in the Si melt is oxidized by Na_2O at the slag-Si interfacial area. The B transferred to the slag is further removed at the slag-gas interface as $Na_2B_2O_4$, which is a more volatile compound than B_2O_3 and $Na_2B_4O_7$ **[49]**. The states in which impurities exist in the slag system is changed by the blown active gas, and the equilibrium state of the B oxidation reaction at the Si-slag interface is broken, promoting the removal of B to a greater extent **[38,42–44,49]**. The addition of a metal melt reduces the activity of Si in Si alloys and improves the B activity coefficient, which can increase the L_B and B removal ratio **[14,28,39,45,47,50]**.

Table 2. Removal of B from Si using different slag systems.

Slags	**Synergism**	**Results**	**Reference**
CaO-SiO_2		→ 0.42 ppmw (seed end)	Liaw *et al.* [15]
		L_B = 5.5 (R = 0.55 - 1.21)	Teixeira *et al.* [16]
		18 → 1.8 ppmw, L_B = 1.57 (R = 1.5)	Wu *et al.* [18]
SiO_2-Na_2O		10.6 → 0.65 ppmw, 0.4→0.2 ppmw	Fang *et al.* [19]
SiO_2-Li_2O		8.6 → 0.4 ppmw	Lai *et al.* [20]
CaO-SiO_2-MgO		L_B = 1.7 (R = 0.95)	Noguchi *et al.* [21]
		→ 10 ppmw	Liaw *et al.* [15]
CaO-SiO_2-Al_2O_3		15 → 2 ppmw, L_B = 4.1	Luo *et al.* [22]
		lg (L_B) = 0.68 - 2.58	Jung *et al.* [23]
CaO-SiO_2-NaO_2		30 → 4.5 ppmw, L_B = 2.4 (R = 1)	Safarian *et al.* [24]
		L_B = 5.81 (R = 1.21)	Zhang *et al.* [25]
CaO-SiO_2-K_2CO_3		22 → 1.8 ppmw, L_B = 2.08 (R = 1)	Wu *et al.* [26]
CaO-SiO_2-BaO		58 → 6 ppmw, L_B = 5.17 (R = 1)	Hou *et al.* [27]
CaO-SiO_2-La_2O_3		→ 4.06 ppmw, L_B = 3.65	Zhu *et al.* [28]
CaO-SiO_2-CeO_2		→ 16 ppmw, L_B = 3.06 (R = 1)	Hou *et al.* [27]
CaO-SiO_2-ZnO		12.94 → 2.18 ppmw, L_B = 3.04 (R = 1)	Wang *et al.* [29]
CaO-SiO_2-Li_2O		18 → 1.3 ppmw, L_B = 1.57 (R = 1.5)	Wu *et al.* [30]
CaO-SiO_2-CaF_2		L_B = 1.6 (R = 2)	Noguchi *et al.* [21]
CaO-SiO_2-LiF		22 → 1.3 ppmw, L_B = 1.6 - 2.7 (R = 0.8)	Ding *et al.* [31]
CaO-SiO_2-$CaCl_2$		148 → 21 ppmw, L_B = 1.36 (R = 1.36)	Wang *et al.* [32]

SiO_2-MgO-Al_2O_3		$L_B = 2.26$	Jakobsson *et al.* [33]
SiO_2-Al_2O_3-Na_2CO_3		7.93 → 0.29 ppmw	Yin *et al.* [34]
CaO-SiO_2-Al_2O_3-CaF_2		25 → 4.4 ppmw, $L_B = 2.29$	Li *et al.* [35]
CaO-SiO_2-MgO-Al_2O_3		$L_B = 1 - 1.8$	Johnston *et al.* [36]
CaO-SiO_2	Cl_2	→ 146 ppm	Nishimoto *et al.* [37]
CaO-$CaCl_2$	Ar-H_2O-O_2	22 → 2.1 ppmw	Xia *et al.* [38]
CaO-SiO_2-Na_2SiO_3	Si-Sn alloy	12.92 → 0.36 ppmw	Li *et al.* [39]
CaO-SiO_2-CaF_2	Si-Sn alloy	→ 0.3 ppmw, $L_B = 200$ ($R = 1.4$)	Ma *et al.* [40,41]
CaO-SiO_2-$CaCl_2$	Ar-O_2	14.7 → 1.94 ppmw ($R = 1$)	Xu *et al.* [42]
	NH_3	75 → 1.5 ppmw ($R = 1.29$)	Chen *et al.* [43]
	Ar-H_2O-O_2	22 → 0.6 ppmw	Wang *et al.* [44]
	Si-Sn alloy	18.36 → 3.7 ppmw ($R = 1.5$)	Al-khazra *et al.* [45]
CaO-SiO_2-Na_2O-Al_2O_3	Si-Cu alloy	$L_B = 46.8$	Li *et al.* [46]
CaO-SiO_2-Al_2O_3-CaF_2	Si-Cu alloy	RE = 80 %	Qian *et al.* [47]

R = [CaO]/[SiO_2]; RE is the removal ratio.

3. Chlorination

Vaporization by reaction with active species containing H-O **[51-53]**, N-H **[54,55],** and Cl **[37]** is another important method for removing impurity elements from Si. Chlorination is distinct because the Cl source can be either a gas or molten salt, and has been employed to remove B from the Si. Nishimoto *et al.* **[37]** investigated the reaction between Si and Cl gas (25 vol.%, mixed with Ar gas) at 1823 K and found no obvious B content change in molten Si. Comparatively, B in the slag was reduced linearly with time and the removal ratio of B was only 2.9×10^{-5} s^{-1}. The results of this study indicated that selective chlorination for B removal could only be applied with a combination of slag refining processes. The corresponding reactions are as follows:

$$B\ (l\ in\ Si) + 0.75O_2\ (g) = BO_{1.5}\ (l\ in\ slag),\quad \Delta G^{\circ} = -664.7+0.13T\ kJ/mol \tag{4}$$

$$4BO_{1.5}\ (l\ in\ slag) + 2Cl_2\ (g) = 4BOCl\ (g) + O_2\ (g),\quad \Delta G^{\circ} = 115.4-0.46T\ kJ/mol \tag{5}$$

Chlorine is a toxic gas that produces corrosive HCl and HClO when reacted with water, and chloride salts have become an alternative method for selective chlorination. The representative reaction is:

$$BO_{1.5}\ (l\ in\ slag) + 0.5CaCl_2\ (l) = BOCl\ (g) + 0.5CaO\ (s),\ \Delta G^{\circ} = 572.2-0.13T\ kJ/mol \tag{6}$$

The calculated partial pressure of BOCl near the surface of the slag was in the range of 10^0–$10^{1.55}$ Pa **[56]**. It should be noted that BOCl was not the only volatile product. The refining process generated $BCl_{x\ (x\ =\ 1,\ 2,\ 3)}$, $SiCl_{x\ (x\ =\ 1,\ 2,\ 3,\ 4)}$, SiO, and $CaCl_2$. Wang *et al.* **[34]** predicted the partial pressures of the potential gas products in the reaction of B-containing Si with CaO-$CaCl_2$ slag and molten Si (**Fig. 2**). Here, the concentrations of Ca and B in molten Si were 200 and 50 ppmw, respectively. The results showed that the ratio of the B-bearing gas to the Si-bearing gas was higher than that of the mole fractions of B and Si. Comparatively, the reaction between the Si-Ca-B melt and Cl_2 generates a gas with a similar elemental ratio as the melt composition. This is why selective chlorination cannot be realized without slag. Boron was removed from Si in two steps with the help of slag, namely oxidation and capture in the slag and chlorination and evaporation. Wang *et al.* **[32]** defined a parameter to evaluate the role of the second step in the refining process, which is the evaporative efficiency of B:

$$\varphi = 1 - {}^{(m_{\mathrm{B\ final\ in\ S}i} + m_{\mathrm{B\ final\ in\ slag}})}\!/_{m_{\mathrm{B\ initial}}} \tag{6}$$

where *m* is the mass content of B. Together with the B removal efficiency and L_B, φ indicates the optimization direction of the chloride-containing slag composition and varies from 2–85% in reported experimental results **[32,57]**. The B removal ratio with $CaCl_2$-containing slag reached 50–96%, as reported by several studies **[32,57-58]**, which is a better B removal ratio than that achieved with Cl gas-blowing refining (21%) **[37]**. Although the use of chloride-containing slag increased the B removal ratio, it could not prevent Si loss during the refining process. The Si loss contributed to the oxidation of Si and the evaporation of Si-bearing volatiles. The Si loss increased with an increase in temperature and reached 22 mass% at 1973 K after refining for 30 min **[57]**, and reached approximately 30 mass% after a prolonged operation time **[58]**.

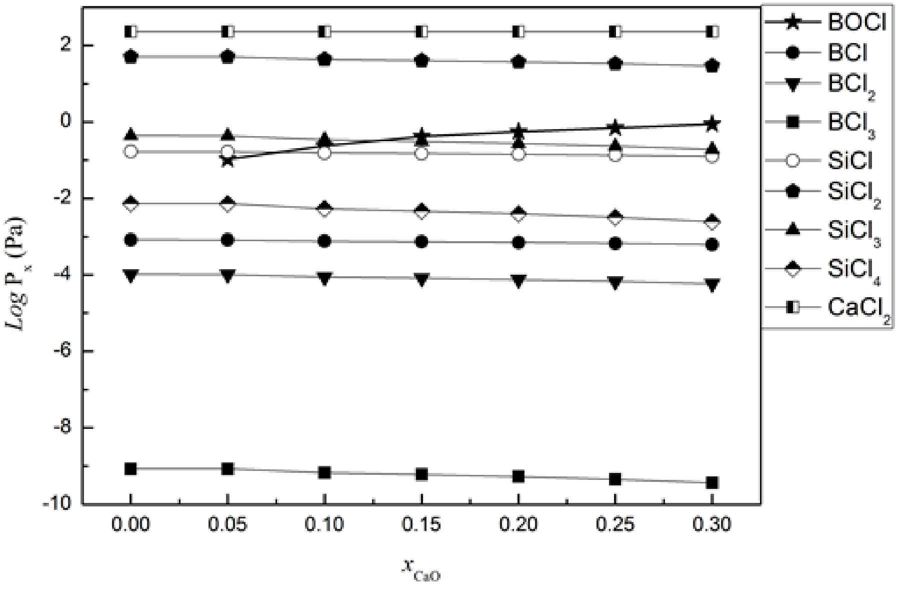

Fig. 2. Thermodynamic prediction of the partial pressures in the chlorination reaction between molten

Si-Ca-B and CaO-$CaCl_2$ slag **[32]**.

Most studies on chlorination refining adopted the CaO-SiO_2-$CaCl_2$ ternary slag system. One exception is the CaO-$CaCl_2$ binary system in the experimental report of Xia *et al.* **[38]**. SiO_2 was generated *in situ* by the oxidation of Si which dissolved into the binary system to form a ternary system at 1823 K. Knowledge of the thermodynamic properties of the slag can assist in optimizing the composition for a larger B removal ratio. Wang *et al.* **[13,59]** measured the density and liquid zone of the slag system. **Figure 3** shows that most of the reported slag compositions were located in the liquidus area of the ternary system at 1723 K. The other points mostly corresponded to the refining temperature at higher temperatures, which ranged from 1723 to 2023 K. The optimum $CaCl_2$ content is approximately 10 mass%, provided the excess $CaCl_2$ can react with SiO_2, thus changing the basicity and hindering the oxidation of B **[60]**.

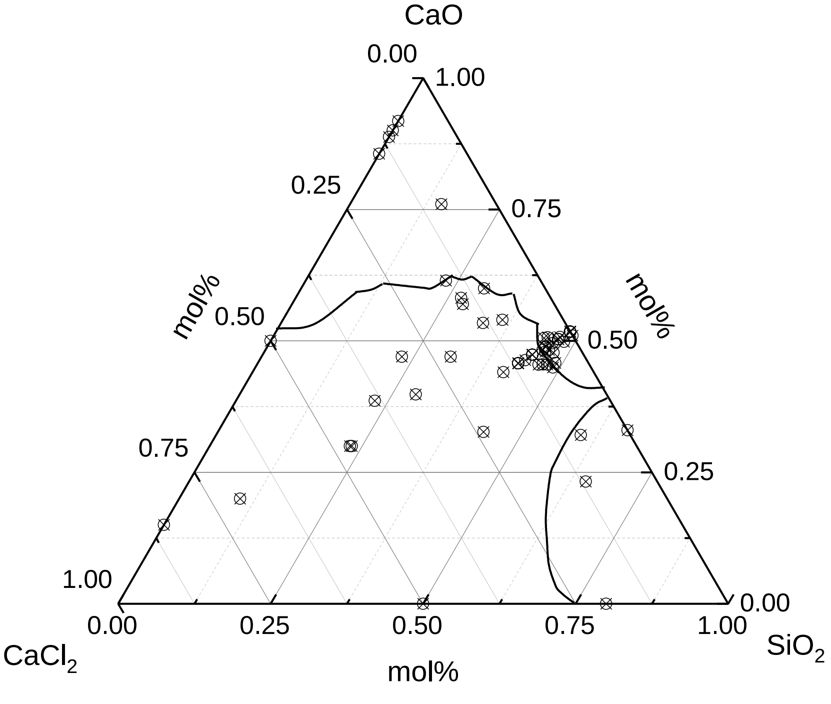

Fig. 3. Reported slag compositions in the selective chlorination refining of Si (the related references are

not cited here, but they are all included in the reference list), where the curve is the liquidus line at 1723 K **[59]**.

Compared to the slag refining process without active components, the selective chlorination process includes several additional kinetic steps in the reaction, namely: (1) the chlorination of $BO_{1.5}$ in the slag; (2) the mass transport of the chlorination products to the slag/gas interface; (3) the evaporation of B-bearing volatiles at the slag/gas interface; and (4) the mass transport of B-bearing volatiles in the gas phase. Usually, step (1), step (4), or diffusion in molten Si is not the rate-determining step in the reaction kinetics at high temperatures **[61,62]**. This implies that the B diffusion coefficient and D_s in the slag determines the reaction rate. It was found that the value of D_s increased from 4.5×10^{-9} to 8.5×10^{-9} m/s^2 with an increase in the $CaCl_2$ content from 10 to 47 mol% in the CaO-SiO_2-$CaCl_2$ slag at 1723 K **[62]**.

Increasing the L_B and φ obviously increases the B removal ratio. The L_B of the CaO-SiO_2-$CaCl_2$ slag maintained the same trend as the slag basicity of the CaO-SiO_2 binary system **[32]**. This indicates that a basicity of approximately 0.8 is optimal for the slag as it reaches the lowest value of L_B. Moreover, an increasing amount of $CaCl_2$ also benefits the formation of BOCl and enhances B removal **[58]**.

In recent years, researchers have reported that the combination of chlorination with alloying **[60,63]** and the combination of selective chlorination and gas blowing further improved the B removal efficiency. A mixture of Ar (20 vol.%), O_2 (40 vol.%), H_2O, and $CaCl_2$ slag (15 mass%, basicity = 1) could remove 96.6% of B from Si in 2 h at 1823 K, which is an improved performance over the single refining processes of chlorination (86%) and oxidation (55.5%) **[64]**. A B removal ratio of 90.5 % was also achieved with CaO (20 mass%)-$CaCl_2$ slag refining combined with Ar (15 vol.%)-O_2 (30 vol.%)-H_2O gas blowing at 1823 K for 3 h **[38]**. In the refining process, BO, HBO, and BOCl were simultaneously generated as gaseous species. Wang *et al.* **[44]** reported a B removal ratio of 96.77% when combining slag chlorination, gas blowing, and a pickling process. Chen *et al.* **[43]** reported a synergistic refining process with CaO-SiO_2-$CaCl_2$ slag and ammonia gas blowing and realized a 98% B removal ratio at 1823 K in 1 h. It should be noted that gas blowing can mechanically stir the melts and accelerate the refining process. The reaction time in the selective chlorination process was reduced from 75 to 5 min with Ar gas stirring **[65]**. As demonstrated, combining chlorination with other technologies is a popular topic in the development of the chlorination process.

4. Vacuum evaporation

Vacuum evaporation is an effective method for purifying Si and is based on the vapor pressure differences of the impurity elements and Si. **Figure 4** shows the standard vapor pressures of the different elements. The figure shows that the typical impurities in MG-Si, such as P, Ca, Mg, Mn, and Al, can be eliminated by vacuum evaporation because their standard vapor pressures are significantly larger than that of Si. Additionally, **Figure 4** also indicates that B and Ti impurities cannot be removed from Si by vacuum evaporation. A large difference in the vapor pressures of the impurity elements and Si, and a large vacuum degree in the atmosphere, indicates an easier removal of impurities from MG-Si through vacuum evaporation. Therefore, the ease of removing impurities by vacuum evaporation can be sequentially ranked from easy to difficult as P > Mg > Ca > Mn > Al > Ti > B, indicating that vacuum evaporation is an effective approach to eliminate P (an impurity which cannot be easily eliminated by other approaches). Notably, the standard vapor pressure gradually increases with an increase in the refining temperature, indicating that an increase in the refining temperature can also enhance the removal of impurities. However, the standard vapor pressure of Si increases quickly with an increase in the refining temperature, as shown in **Fig. 4**, indicating that a trade-off on the mass loss of Si exists when increasing the refining temperature to enhance the removal of impurities.

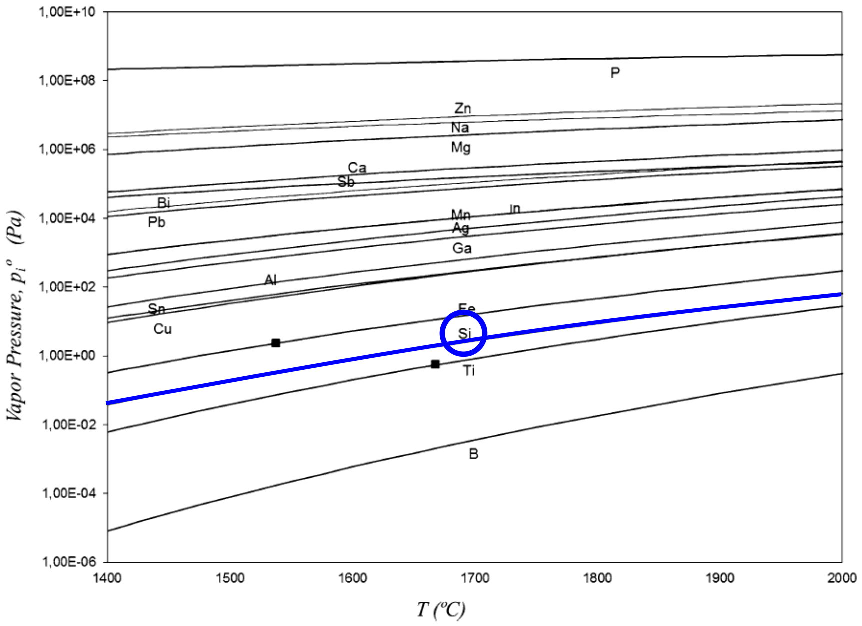

Fig. 4. Standard vapor pressure of various elements in Si **[66]**.

Safarian *et al.* **[66]** investigated the removal of P by vacuum evaporation and demonstrated that P removal was controlled by both the chemical reaction and mass transfer in the gas phase, and the P removal ratio significantly increased with an increasing temperature. Jiang *et al.* **[67]** performed P removal using directional solidification technology under vacuum (<0.1 Pa). The P removal ratio was dependent on the refining temperature and solidification rate, and 85% P could be eliminated at 1823 K when the solidification rate was 1.97×10^{-6} m/s. Zheng *et al.* **[68]** established a numerical model of P evaporating from Si and demonstrated the decreasing sequence of factors influencing the removal of P as temperature, pressure, geometry of the Si melt, refining time, and initial P concentration. Additionally, an increase in the removal of P normally results in an increase in the mass loss of Si. For example, the Si yield decreased from 99.14 to 90.5% when the residual concentration of P in Si decreased from 10.29 to 0.11 ppmw **[68]**. Hoseinpur *et al.* **[69]** studied the evaporation of P from liquid Si under vacuum and reduced H_2, He, and Ar pressures to evaluate the feasibility of effectively removing P with a minimal Si loss. They found that the introduction of the inert gases of Ar and He at low pressures reduced the P removal ratio, and their pressure decrease increased the processing rate. Their recent study **[70]** examined the application of ultra-high temperatures, up to 2173 K, for the removal of P from Si in a vacuum-induction refining process. The results showed that P was completely removed in a short duration from Si melts with P concentrations as high as 92.71 ppmw when the vacuum was approximately 7 Pa.

Vacuum evaporation was also used to remove impurities other than P. Wei *et al.* **[71]** conducted experiments to eliminate Al from Si at 1823 K and 10 Pa, and the Al removal ratio was 61.9% (the concentration of P decreased from 1120 to 427 ppmw) when the refining time was 90 min. Tan *et al.* **[72]** eliminated Al and Ca from Si by a combination of vacuum induction melting and directional solidification, and demonstrated that the removal of Al and Ca mainly depends on their evaporation in the vacuum induction melting process, with the refining temperature and vacuum degree being the main factors influencing the removal of impurities. Ren *et al.* **[73]** used low-vacuum directional solidification (6×10^{-4} Pa at 1687 K) to eliminate Cu, Mn, and Na from Si. Copper and Mn were mainly eliminated by directional solidification, and their concentration in Si decreased from 28.56 to 0.1 ppmw and 10.53 to 0.01 ppmw, respectively, while Na was mainly eliminated by vacuum evaporation, and its concentration decreased from 1096.91 to 0.2 ppmw.

5. Solvent refining

Solvent refining is a low-temperature Si purification technology that can refine Si below its melting point. The mechanism of solvent refining is similar to directional solidification, that is, impurities can be eliminated from Si by the segregation behaviors of impurities at the liquid/solid interface. Therefore, the segregation ratio, $k_i = C_{i \text{ in solid Si}}/C_{i \text{ in the liquid melt}}$ (the concentration ratio of the impurity, *i*, in solid Si to that in the liquid melt), is the key factor for eliminating impurities from Si by solvent refining. The segregation ratios of impurities decreased with a decrease in the melting point of the solvent. Therefore, solvent refining with a low refining temperature not only purifies Si with a low energy consumption but also removes impurities with high removal ratios. In solvent refining, Si is the solute and one or more other elements are used as solvents. The elements that can be used as solvents should have the following characteristics:

(1) the solubility of the solvent element (such as Cu and Fe) in solid Si is extremely low, or the solvent element (such as Al and Sn) dissolved in solid Si can be easily removed by vacuum evaporation or other methods. This characteristic ensures that the solvent element cannot contaminate the refined Si crystals;

(2) are low cost (or recyclable) and environmentally friendly;

(3) the solvent element and the Si solute can form a low-melting point liquid melt, or have a low eutectic temperature (such as Si-Al, Si-Ga, and Si-Cu). This characteristic enables Si purification at a temperature that is considerably lower than the melting point of pure Si (1687 K); and

(4) the concentration of the solvent element (such as Al, Sn, Ga) at the eutectic point in the phase diagram should be as small as possible, which can result in a high yield of purified Si crystals, and only a small amount of Si is lost after solvent refining.

Many Si-based solvents have been proposed for Si purification based on the characteristics of the solvent elements mentioned above.

5.1 Si-Al solvent

Aluminum is chosen as the solvent for Si purification because of its advantages, namely (1) the Al-Si system has a low eutectic temperature of 850 K **[74]**; (2) Al is a widely used and cheap metal; (3) after separating the purified Si crystals from the Al-Si solvent, the residual Al-Si alloy is an eutectic Al-Si alloy which can be directly used as a raw material to prepare Al-Si alloys (recyclable); (4) the segregation ratios of B and P impurities, which cannot be easily eliminated, are significantly decreased; and 5) the concentration of Al in the eutectic Si-Al alloy is 12.2 at.% (850 K) **[74]**, indicating a large yield of refined Si crystals.

Table 3 Evaluated segregation ratios of impurity elements between the Si-Al melt and solid Si **[75-78]**.

Element	Segregation ratios			Segregation coefficients
	1073 K	1273 K	1473 K	1687 K
Fe	1.7×10^{-11}	5.9×10^{-9}	3.0×10^{-7}	6.4×10^{-6}
Ti	3.8×10^{-9}	1.6×10^{-7}	9.6×10^{-7}	2.0×10^{-6}
Cr	4.9×10^{-10}	2.5×10^{-8}	2.5×10^{-7}	1.1×10^{-5}
Mn	3.4×10^{-10}	4.5×10^{-8}	9.9×10^{-7}	1.3×10^{-5}
Ni	1.3×10^{-9}	1.6×10^{-7}	4.5×10^{-6}	1.3×10^{-4}
Cu	9.2×10^{-8}	4.4×10^{-6}	2.5×10^{-5}	8.0×10^{-4}
Zn	2.2×10^{-9}	1.2×10^{-7}	2.1×10^{-6}	1.0×10^{-5}
Ag	1.9×10^{-8}	1.7×10^{-6}	6.6×10^{-6}	1.7×10^{-5}
Au	1.5×10^{-11}	6.1×10^{-9}	3.6×10^{-7}	2.5×10^{-5}
Ga	2.1×10^{-4}	8.9×10^{-4}	2.4×10^{-3}	8.0×10^{-3}
In	1.1×10^{-5}	4.9×10^{-5}	1.5×10^{-4}	4.0×10^{-4}
Sb	3.4×10^{-3}	3.7×10^{-3}	8.2×10^{-3}	2.3×10^{-2}

Pb	9.7×10^{-5}	2.9×10^{-4}	1.0×10^{-3}	2.0×10^{-3}
Bi	1.3×10^{-6}	2.1×10^{-5}	1.7×10^{-4}	7.0×10^{-4}
P	4.0×10^{-2}	8.5×10^{-2}	1.6×10^{-1}	3.5×10^{-1}
B	7.6×10^{-2}	2.2×10^{-1}	4.9×10^{-1}	8.0×10^{-1}
Al	1.4×10^{-4}	4.9×10^{-4}	1.2×10^{-3}	2.8×10^{-3}
Hf	-	2.3×10^{-6}	6.2×10^{-6}	4.9×10^{-6}

Obinata and Komatsu proposed Si-Al solvent refining in 1957. Kazuki and Yoshikawa investigated the thermodynamic data for the Si-Al solvent refining of MG-Si and obtained positive results for Si purification. According to **Table 3 [75-78]**, the segregation ratios of the B and P impurities can be significantly decreased. This important thermodynamic investigation provided important information to solve the bottleneck, that is, effectively eliminate B and P from Si. Therefore, Si-Al solvent refining technology has attracted the attention of researchers and is now becoming the most common solvent refining technology for Si purification.

However, Si-Al solvent refining has some disadvantages, namely (1) the density of Al is close to that of Si (2.3 g/cm^3 for Si and 2.7 g/cm^3 for Al), indicating that the purified Si crystals cannot be easily separated from the Si-Al melt by gravitational separation; acid leaching out Al is an effective method, but the Al solvent cannot be recycled and (2) although Si-Al solvent refining can enhance the removal ratios of B and P, it is difficult to control the concentrations of B and P to <1 ppm.

To address the first disadvantage, Morita and Yoshikawa **[79]** proposed the separation of purified Si crystals from the Si-Al solvent with the assistance of electromagnetic force, as shown in **Fig. 5 [79]**. This approach reduced the acid consumption and the loss of Al in the acid leaching process. Zou *et al.* **[80]**

investigated the effects of the temperature gradient and electromagnetic stirring on the separation of Si crystals from the Al-Si melt and obtained a Si-rich layer with 65–70 wt.% Si. Lv *et al.* **[81]** demonstrated that the separation of Si from the Al-Si solvent by electromagnetic directional solidification depends on the Si growth rate and the solidification rate of the melts. Jiang *et al.* **[82]** obtained the morphological evolution of Si during the electromagnetic directional solidification as the planar → cellular → columnar → dendritic stages. In addition to electromagnetic separation, Li *et al.* **[83]** proposed using super gravity to separate Si crystals from the Al-Si solvent. **Figure 6** shows the equipment used. The Si crystals were efficiently separated from the Al-Si solvent with an optimum gravity coefficient of 280. Nishi *et al*. **[84]** used directional solidification with resistance heating to separate Si from the Al-Si solvent by preparing bulk Si, as shown in **Fig. 7**. Li *et al*. **[85]** used the modified Czochralski method to separate Si from the Al-Si melt (**Fig. 8**).

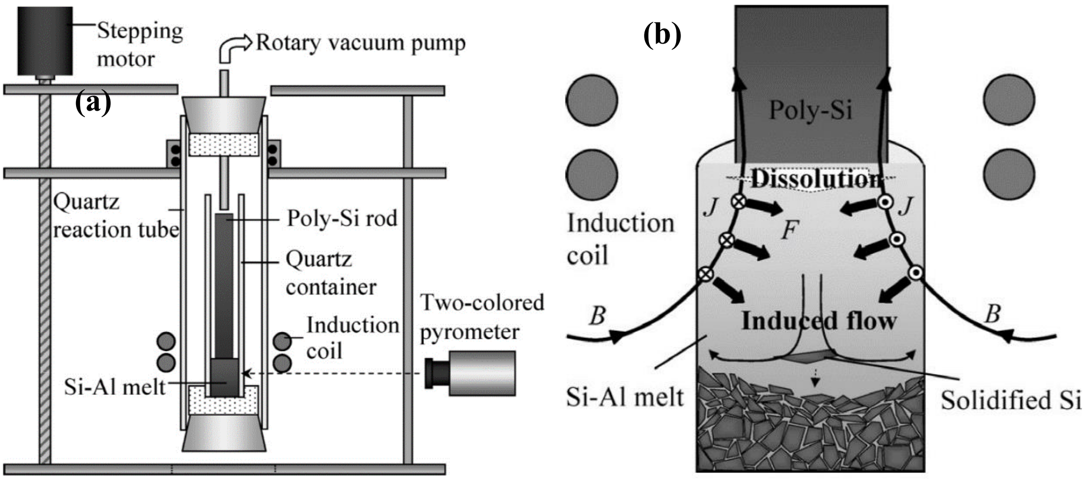

Fig. 5. (a) Equipment used for the separation of the Al-Si melt with the assistance of an electromagnetic force and (b) the electromagnetic separation mechanism **[79]**.

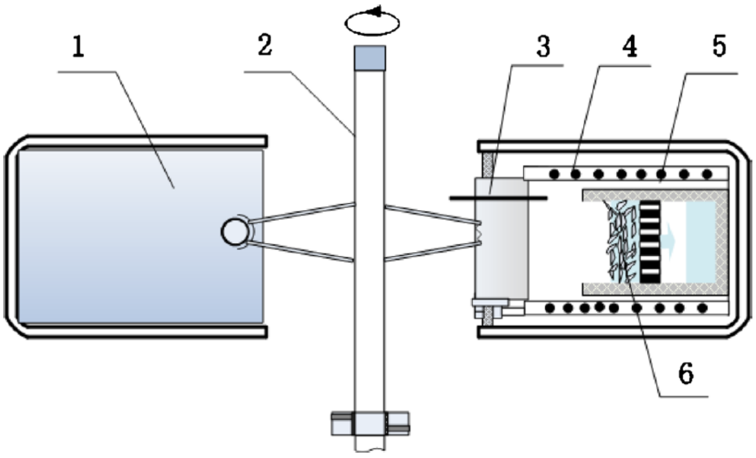

Fig. 6. Equipment used for the separation of Si from the Si-Al solvent by super gravity **[83]**. 1. Counterweight; 2. centrifugal axis; 3. thermocouple; 4. resistance coil; 5. alumina filter; and 6. specimen.

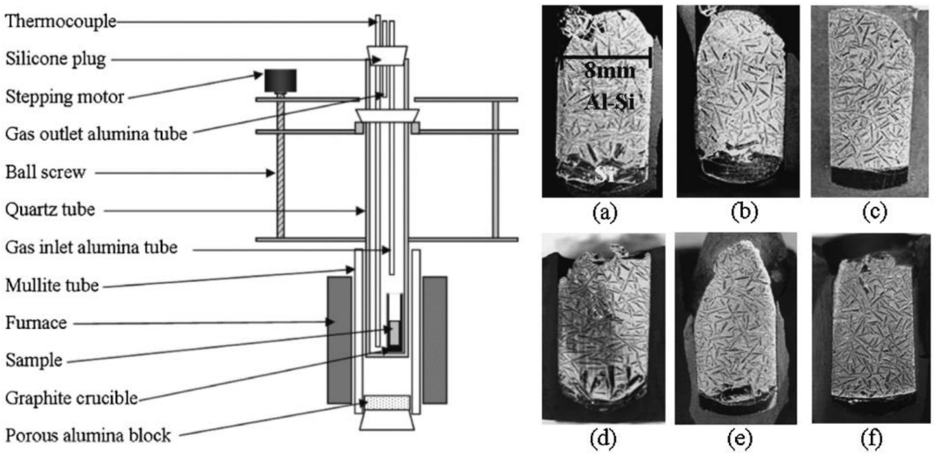

Fig. 7. Equipment used for the separation of Si from the Si-Al solvent by directional solidification with resistance heating; and the samples with a temperature gradient of 1.5 K/mm and a cooling rate of (a) 0.105, (b) 0.084, and (c) 0.031 K/min; and the samples with a temperature gradient of 4.0 K/mm and a cooling rate of (d) 0.273, (e) 0.194, and (f) 0.08 K/min. **[84]**.

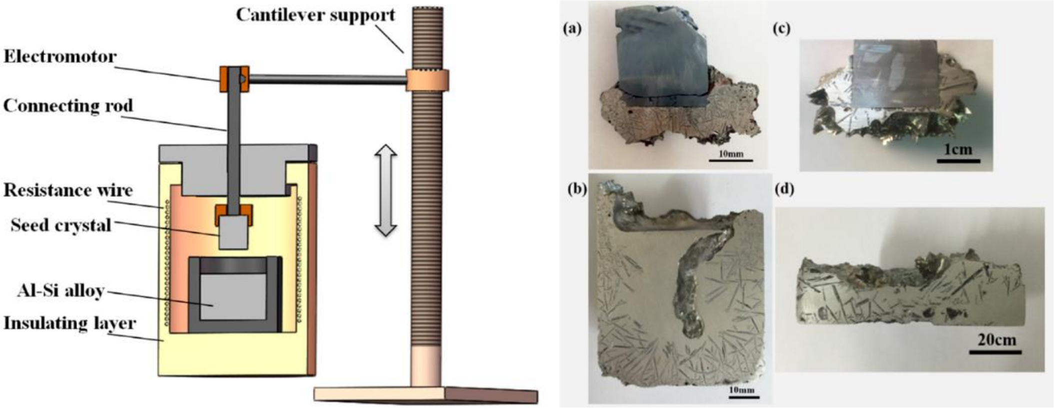

Fig. 8. Equipment used for the separation of Si from the Si-Al solvent by the modified Czochralski method, and the obtained samples of the (a) pulled-up alloy and (b) alloy remaining in the Al-25%Si solvent; (c) pulled-up alloy and (d) alloy remaining in the Al-28%Si solvent **[85]**.

To address the second disadvantage, Morita and Yoshikawa **[86]** proposed using Ti as an additive to enhance the B removal ratio using a Si-Al solvent because Ti has a strong affinity for B and Ti and B form TiB_2 in the Si-Al solvent. Bai *et al*. **[87]** and Ban *et al*. **[88]** removed B with a Ti addition using an Al-30%Si solvent, and the concentration of B in Si could be decreased to <1 ppmw with a 2000 ppmw Ti addition. Lei *et al*. **[89]** found that the affinity of Zr and Hf for B is stronger than that of Ti for B, and proposed using Zr, Hf, and V as new B getters to enhance the removal of B from Si using a Si-Al solvent. They demonstrated that the concentration of B in the Si could be easily controlled to <1.6 ppmw with the addition of small amounts of Zr and Hf (<1100 ppma), and the addition of Zr and Hf enabled a higher B removal ratio than the addition of Ti, as shown in **Fig. 9 [89]**. The mechanism of B removal with the addition of Zr to the Al-Si melt is the formation of ZrB_2, which decreases the equilibrium concentration and segregation ratio of B, as shown in **Fig. 10 [90]**. However, the added Zr, Hf, and V could not be easily removed by a mixture of H_2SO_4 and aqua regia. Lei *et al*. **[91]** further increased the added amounts of Zr, Hf, or Ti (Al-45 at.% Si with 1 at.% Zr, Hf, or Ti) to enhance the removal of B, and proposed using a mixture of HCl + HF to remove the Zr-, Hf-, or Ti-containing phases. They demonstrated that the residual B concentration in purified Si was <1 ppmw, and the removal ratios of the added Zr, Hf, and Ti were 99.998%, 99.9994%, and 99.997%, respectively. Chen *et al*. **[92]** used the same acid mixture to remove the added V, and the V removal ratio was nearly 100% (below the detection limit of ICP-OES). Yu *et al*. **[93]** also reported that HF is a better leaching agent than aqua regia for leaching Ti-containing phases. Therefore, the addition of Zr, Hf, Ti, or V can enhance the removal of B in an Al-Si solvent, and all of them can be easily removed during the Si refining process. Aluminum-Si solvent refining with Zr, Hf, Ti, or V additives can be described as "enhancing impurity removal with impurities," specifically, "using the easily-removed metallic impurities to enhance the removal of difficult-to-remove non-metallic impurities." Chen *et al*. **[94-95]** obtained a 99.36% B removal rate using slow cooling solidification refining of an Al-30wt.% Si solvent with Zr additions, and investigated the impurity phase migration during directional solidification.

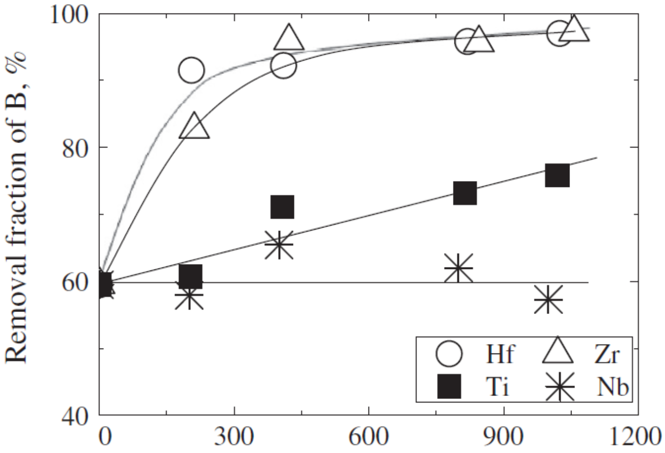

Fig. 9. Boron removal after the electromagnetic solidification purification of Si using Al-Si solvent refining with additives (ppma) **[89]**.

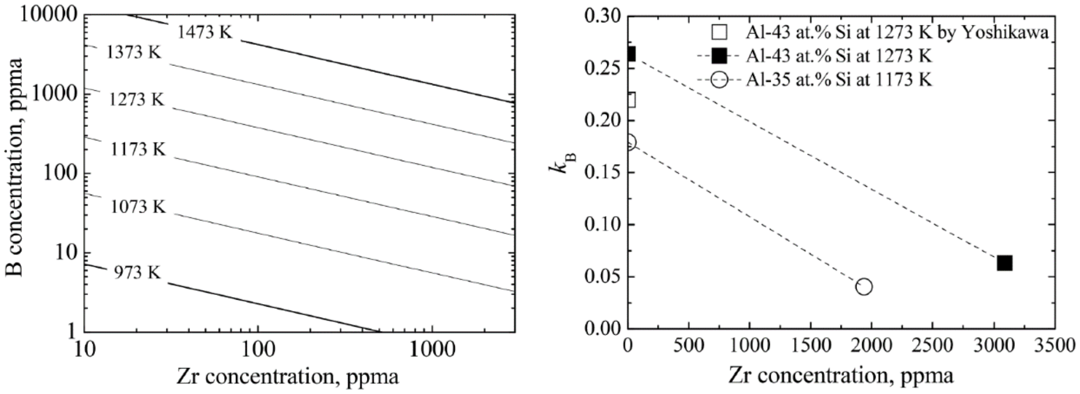

Fig. 10. (a) The relation between the equilibrium concentrations of Zr and B in the Si-saturated Al-Si melt and (b) the effect of Zr additions on the segregation ratio of B in the Si-saturated Al-Si melt **[90]**.

Besides adding Zr, Hf, and Ti additives, Li *et al.* **[96]** used mechanical stirring to enhance the removal of impurities in Al-Si solvent refining. Zou *et al.* **[97]** demonstrated that the effective segregation coefficients of B and P could be decreased using electromagnetic stirring, and the concentrations of B and P in Si decreased with an increasing magnetic field intensity. He *et al.* **[98]** determined that the concentrations of the Fe, Ti, Ca, and B impurities decreased with a decreasing initial Si content in the Al-Si solvent. Xiao *et al.* **[99]** enhanced the removal of Fe from Si by adding Mn, and the Fe removal efficiency was 90%. Qian *et al.* **[100]** demonstrated that 99.5% of metallic impurities were eliminated in bulk-grown bulk silicon. Ban *et al.* **[101]** investigated the purification of Si with Al-Si solvent under a rotating electromagnetic field with varying frequencies, and the apparent segregation coefficients of B and P were determined as 0.12 and 0.06, respectively.

5.3 Si-Sn solvent

The Si-Sn binary system was chosen as the solvent for Si purification because of its very low eutectic temperature (505.08 K) in which the Si concentration at the eutectic point is only 4×10^{-5} at.%, the solubility of Sn in solid Si is low (the largest value is <0.1 at.%), and no Si-Sn intermetallic compound is formed **[102]**. The residual Sn in the refined Si after solvent refining can be easily removed by high-temperature vacuum treatment because the vapor pressure of Sn is significantly larger than that of Si. Additionally, SoG-Si can tolerate a Sn concentration of 10 ppmw because it is an electrically inactive element **[75]**. However, the Si-Sn system has a moderate liquidus slope, which indicates that a large amount of Si will precipitate when the Si-Sn alloy is cooled between 1673 and 1573 K. This refining temperature range is higher than that of the Si-Al system, given the similar Si yield. Therefore, the distribution coefficient of impurities between Si and a Si-Sn melt is significantly higher than that between Si and a Si-Al melt. Zhao *et al.* **[103]** reported that the B segregation coefficient decreased to 0.038 at 1500 K when the refining temperature was lower, which is significantly lower than the 0.8 at the Si melting point.

Ma *et al.* **[104]** measured the thermodynamic properties of B in the Si-Sn system by the equilibration of a liquid alloy with a B solid solution or Si boride at 1673 K. The activity coefficient of B in the Si-Sn melt was three orders of magnitude larger on the Sn-rich side than on the Si-rich side (**Fig. 11**). This thermodynamic instability is a unique feature of the Si-Sn solvent which allows for the easy removal of B. The large activity coefficient of B in the Si-Sn solvent indicates that the combination of Si-Sn solvent refining and slag treatment can enhance B removal according to **Eq. (2)**. Ma *et al.* **[41]** proposed a method for the removal of B from Si by slag treatment with a Sn addition. By adding Sn to the Si phase, the B activity coefficient was dramatically increased, while the O partial pressure decreased. Both factors lead to an even higher L_B than the normal slag treatment of the Si phase. To date, the obtained L_B is the highest value achieved in the slag treatment of Si and other Si-based solvents **[105,106]**. Li *et al.* **[39]** investigated the effect of the slag treatment parameters on the removal of B using basic slag with Na_2O. Al-khazraji *et al.* **[50]** changed the slag system to CaO-SiO_2-$CaCl_2$ to facilitate the B removal by forming B oxy-chloride (BOCl) gas. Hafnium, Zr, and Ti were added to the Si-Sn solvent to remove B by the formation of boride, because B becomes more thermodynamically unstable in the Si-Sn melt, and Hf, Zr, and Ti have a strong affinity for B **[107,108]**. Boron can be removed to some extent but is limited because of the relatively high refining temperature. In addition to B removal, Hu *et al.* studied the removal of P from a Si-Sn solvent with a Ca addition and demonstrated that the P removal ratio increased from 73.4 to 86.5% when Ca was added to the Sn–Si refining system. A P-rich phase with up to 17.8% P was identified in the refined Si after the Sn–Si refining process with a Ca addition **[109]**.

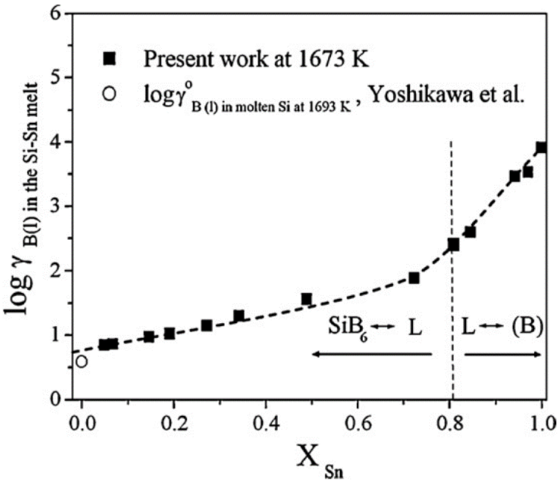

Fig. 11. Activity coefficient of B in the Si-Sn melt at 1673 K **[104]**.

The separation of refined Si from the Si-Sn solvent is as equally important as the purity of refined Si to achieve a high as possible growth rate and enrich the Si. Ma *et al.* **[110]** studied the Si growth from a Si-Sn solvent by directional solidification. Bulk Si was favored, but the growth rate was very low, on the order of 10^{-7} m/s, because the diffusion coefficient of Si is relatively low, on the order of 10^{-9} m^2/s **[111]**. Zhang *et al.* **[112]** added a Si feed source on top of the melt to keep the Si-Sn solution saturated with Si atoms, and the growth rate of Si was increased by approximately three-fold. Ren *et al.* **[113]** changed the directional solidification direction for Si growth yielding bulk Si, and the primary Si could float upwards into the mushy zone (supercooling) owing to the large density difference between Si and Sn. Ma *et al.* **[114]** compared the effect of cooling conditions on Si growth from a Si-Sn solvent. The separation efficiency of refined Si achieved by the synergy of slow cooling and electromagnetic stirring flow enrichment was considerably higher than that of directional solidification without compromising the purification efficiency of refined Si. Huang *et al.* **[115]** employed electromagnetic semi-continuous directional solidification to separate and purify Si from a Sn-30Si alloy. The primary Si was enriched to approximately 91% when the solidification rate was 2.5×10^{-4} m/s. Li *et al.* **[116]** proposed a different separation method for refined Si using gas pressure filtration. The optimal results for separation were obtained at p = 0.3 MPa, T = 523 K, and X_{Si} = 20% where 93.6% of Sn was separated into the filtrate, while almost all the Si was recovered.

5.3 Si-Fe solvent

The Si-Fe solvent has been used because of the low cost of Fe and its extremely low solubility and segregation coefficient in Si (6.4×10^{-6} as listed in **Table 3**), which indicates that the contamination of Fe in Si, as a solute, can be minimized. In contrast, the by-products of ferrosilicon alloys are marketable alloys for the steelmaking industry, meaning that the loss of Si in the residual Si-Fe alloy after solvent refining is recyclable.

Leili *et al.* evaluated the thermodynamic properties of B and P removal using a Si-Fe solvent **[117-120]**. The B segregation ratio between solid Si and the Si-Fe melt increased with the B content and temperature. Due to the solvent refining temperature being lower than the melting point of pure Si, the segregation ratios of B, namely 0.49 ± 0.01 at 1583 K, 0.41 ± 0.03 at 1533 K, and 0.33 ± 0.04 at 1483 K, are lower than the equilibrium value of 0.8 for pure Si, but still in the same order of magnitude range. In addition to B, the segregation ratios of P between solid Si and the Si-Fe melt were determined to be 0.22 ± 0.02 at 1583 K, 0.29 ± 0.02 at 1533 K, and 0.33 ± 0.02 at 1483 K, which are lower than the equilibrium value of 0.35 for pure Si. The very large negative interaction coefficient of P on Fe in the Si-Fe melt is -3460 ± 155 at 1583 K, -3595 ± 159 at 1533 K, and -3694 ± 119 at 1483 K, indicating that Fe is a strong gettering solvent to attract P. Therefore, the removal of P from Si in the presence of Fe is more difficult than Si under vacuum conditions **[121]**.

The addition of a third element to the Si-Fe solvent and slag treatment to enhance the removal of B and P was examined. Sakiani *et al.* **[122]** added Ti to a Si-Fe solvent to remove B and P. The reduction of B and P was attributed to the formation of the $Ti_5P_{3.16}$/TiFeP phase and TiB_2. Deng *et al.* **[123]** also confirmed the enrichment of P in the Fe-Si-Ti phase with Ti additions, which enhanced the removal of P by subsequent acid leaching. Although the thermodynamic properties of B and P in the Si-Fe alloy did not show a solid favorable for slag treatment, Leili explored the removal of B and P by combining solvent refining and slag treatment **[124-126]**. A higher slag basicity and O potential resulted in a higher B removal. The highest B partition ratio value (11.42) between the $CaO\text{-}SiO_2\text{-}Al_2O_3$ ternary slags and the Si-Fe alloy was obtained at 1873 K. The highest P partition value (0.1) between the $CaO\text{-}SiO_2\text{-}Al_2O_3$ ternary slags and the Si-Fe alloy was observed at 1873 K. Na_2O was added to form a $CaO\text{-}SiO_2\text{-}Al_2O_3\text{-}Na_2O$ quaternary slag system to eliminate P from a Si-20 wt% Fe alloy at 1300 °C. The maximum partition value for P was 1.19 at a CaO/SiO_2 ratio of 1.36, SiO_2/Al_2O_3 ratio of 1.56, and the addition of 10 wt.% Na_2O. As mentioned above, because of the very large negative interaction coefficient of Fe on P in the Si-Fe melt, the strong affinity of Fe to P limits the removal of P from Si during slag treatment.

Refined Si was recrystallized from Si-Fe alloys and required separation by acid leaching to remove impurities. Esfahani and Barati **[127]** studied the growth of primary Si from a Si-Fe melt under different cooling rates and quenching above the eutectic temperature. The refined Si was recovered using the gravity-based flotation method after grinding. The removal of some typical impurities from the initial MG-Si to refined Si after acid leaching were listed as Fe: 3108 → 1 ppmw, Al: 980 → 10 ppmw, Mn: 158 → 3 ppmw, Ni: 118 → 1 ppmw, B: 27 → 2 ppmw, and P: 68 →29 ppmw **[128]**. Li *et al.* **[129,130]** studied the growth of bulk Si from a Si-Fe melt by directional solidification under different temperature gradients.

5.4 Si-Cu solvent

Copper was chosen as the solvent for Si purification because of its extremely low solubility in solid Si (maximum solubility of 0.002 at.% between 1473 K and 1573 K) and its low eutectic temperature (1075 K) in the Si-Cu system **[131]**. Additionally, the segregation coefficient of Cu in Si is extremely small (8.0×10^{-4}), as listed in **Table 3**.

Because it is difficult to separate purified Si crystals from an Al-Si solvent by gravity, Mitrašinović and Utigard **[132]** proposed using Cu as a solvent to refine Si, because the solubility of Cu in solid Si is relatively small, and Cu has a strong affinity for many elements. The results demonstrated that the concentration of nine elements (namely, Ba, Co, Cr, Mn, Mo, Ni, Sc, Zn, and Zr) in the purified Si was decreased the below the ICP detection limit. Huang *et al.* **[133]** enhanced the B and P removal (21 to 58.7% for B and 23.2 to 42.2% for P) by combining Cu alloying and aqua regia leaching, and obtained a B removal of 85% using a Cu-50wt%Si solvent with a 5% Ti addition **[134]**, a P removal of 82% using a Cu-50wt%Si solvent with a 5% Ca addition **[135]**, and decreased the concentrations of B and P from 3.12 to 0.35 ppmw and 17.14 to 7.27 ppmw, respectively, by the combination of a Cu-50wt%Si solvent and a 45 wt% CaO–45 wt% SiO_2–10 wt% $CaCl_2$ slagging treatment **[60]**. Fang *et al.* **[136]** reported that the Si-Cu solvent was beneficial for the removal of Fe, Al, and Ca from Si. Ren *et al.* enhanced B removal by using a Si-Cu melt with Zr additions **[137]** and obtained a B removal efficiency of 93.4% **[138]**. Chen and Morita **[55]** obtained an 80% B removal rate by combining a Si-Cu solvent and an ammonia-containing gas. Li *et al.* **[46]** investigated the distribution coefficient of B and P between the slag and Si-Cu solvent, and demonstrated through a thermodynamic evaluation that the addition of Cu to the Si-Cu solvent enhanced the removal of B and P.

5.5 Other solvents

Morito *et al.* **[139,140]** proposed the use of a Si-Na solvent for Si purification, and the purified Si crystals could be precipitated by Na evaporation from the Na-Si solution at 1173 K. The concentrations of B and residual Na in the Si decreased to 0.3 ppm **[139]** and 0.055 ppmw, respectively, by vacuum evaporation at 1723 K **[140]**. However, the evaporation of Na made the B removal unstable, and impurities re-contaminated the purified Si. Li *et al.* **[141]** proposed the use of Ga as a solvent for Si refining, and the B and P removal ratios were 83.28% and 14.84%, respectively, with the addition of 25% Ga, but the high cost and recyclability of Ga after Si-Ga solvent refining became a problem. Zhang *et al.* **[142]** combined Si-Al-Ca solvent refining with CaO-CaF_2 slag treatment and obtained a high P removal ratio (98.6%). Li *et al.* **[143]** proposed Si-Al-Zn solvent refining, and the solid-state back-diffusion of impurities was controlled by the addition of Zr to the Al-Si solvent. Si-Al-Sn solvent refining was also proposed to enhance B removal from Si and increased the recovery rate of primary Si **[144,145]**. Additionally, small amounts (normally no more than 5 mass%) of Ti **[146]**, Zr **[147]**, Hf **[9]**, and V **[148]** were directly added to MG-Si to enhance the removal of impurities. The addition of Ti, Zr, Hf, and V can enhance the removal of metallic impurities while significantly enhancing B and P removal. Ren *et al.* **[149]** used a Si-Sn-Cu ternary solvent to refine Si and obtained bulk Si (the bulk Si was enriched to 99.2%), and the B removal ratio was 95.3% with the Zr additions. They also proposed using high-entropy alloys, namely ZrTiHfCuNi, to enhance B removal from Si, because Zr, Ti, Hf, and Ni have a strong affinity for B in high-entropy alloys, and can form borides, such as $(Ti_{3-x}Zr_x)B_4$ or Ni_3B **[150]**. Mei *et al.* **[151]** used Si-Mg solvent refining and obtained Si with a purity of 99.995%. Most of the B, P, Fe, Ca, Ti, Ni, V, and Cu contents were lowered to <1 ppmw. Zhu *et al*. **[152,153]** positively eliminated P and other impurities from Si by using a Si-Ca-Mg solvent (using Ca and Mg as additives).

6. Outlook and conclusions

Based on the comprehensive literature review related to upgrading MG-Si to SoG-Si by pyrometallurgical routes, the following conclusions and future outlooks have been drawn:

(1) Although slag treatment exhibits positive results for B removal, waste slag will be generated if the concentration of B in Si is controlled to an acceptable level for SoG-Si because the value of L_B is normally below 6. Additionally, dozens to hundreds of ppmw of impurities, such as Ca, Al, Mg, and others, still remain in the residual Si because of the equilibrium between the molten slag and the Si melt. If slag treatment is only used to remove B from MG-Si, recycling the waste slag is also a major problem. However, slag treatment has recently been used to remove the SiO_2 impurity layer from diamond wire saw Si powder waste (a type of Si kerf slurry waste) **[154-156]**, which provides an important way to eliminate O and oxides (glasses in spent solar cells) from Si wastes, and the waste slag after removing SiO_2 is a promising recyclable material.

(2) Chlorination can effectively eliminate B from MG-Si, but the slags always contain chlorides that can easily corrode furnace slag, and the evaporable chlorides require careful treatment to protect equipment and to avoid environmental pollution. Additionally, the treatment of chlorides remaining in the residual slag is a major problem. Therefore, chlorination has more environmental problems than other approaches, such as vacuum and solvent refining, and further studies are required to solve these problems.

(3) Vacuum evaporation is a useful and pure physical approach to eliminate volatile impurities from MG-Si. Furthermore, vacuum evaporation is suggested to eliminate the residual volatile impurities in purified Si after slag treatment (such as Ca, Al, and Mg) and solvent refining (such as Al and Sn after Si-Al and Si-Sn solvent refining). Therefore, the optimal utilization of the vacuum approach is worth further study.

(4) Solvent refining using metallurgical routes is the most popular research topic for Si refining because of its low energy consumption and large impurity removal ratios. Obtaining bulk high-purity Si after solvent refining is also a popular research topic and needs to be further investigated. Compared to other solvent refining approaches, Si-Al solvent refining has attracted more attention because of its advantages, namely (a) both B and P can be eliminated effectively; (b) the purified Si crystal can be agglomerated by electromagnetic directional solidification and the residual Si-Al solvent after refining Si with electromagnetic separation is the eutectic Al-Si alloy, which can be recycled as Al-Si alloy castings (the impurities in the residual Si-Al solvent are acceptable because the concentration of Fe in MG-Si is normally <4000 ppmw); and (c) B in Si can be reduced to < 0.1 ppmw with small additions of Zr, Hf, and Ti, and these additives can be simultaneously eliminated without secondary contamination of Si (even if very small residual amounts of Zr, Hf, or Ti (less than 1 ppmw) are present in the purified Si, they can be easily reduced to below 0.0001 ppmw in the next directional crystallization step because of their extremely small segregation coefficients).

(5) **Figure 12** proposes a pure physical approach to prepare SoG-Si and recycle Si waste (Si kerf slurry waste or spent Si-based solar cells). It is suggested that MG-Si can be upgraded to SoG-Si by a combination of solvent refining and vacuum directional solidification. It is also suggested that Si waste can be recycled to SoG-Si by slag treatment to remove oxides, and the Si obtained after slag treatment

can be upgraded to SoG-Si by combining solvent refining and vacuum directional solidification, or only by vacuum directional solidification, depending on the concentration of the B and P impurities in the Si obtained after slag treatment. The pure physical approach is considered an environmentally friendly approach because no waste gas or acidic solution is generated. Although oxide slag is used to remove oxide impurities in the Si wastes, it can be recycled by re-adjusting the composition of the slag. Electric power consumption is the only major problem, but it is acceptable when cheap and green hydroelectric power is employed.

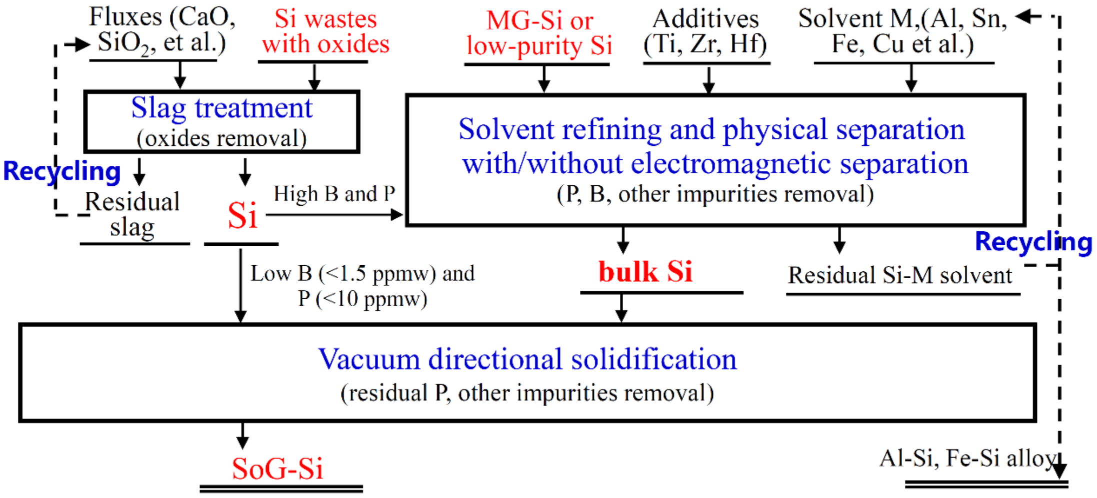

Fig. 12. A pure physical approach is suggested to upgrade MG-Si to SoG-Si or recycle Si wastes as SoG-Si.